

## Article

# Enhanced Adaptive Neuro-Fuzzy Inference System Using Reptile Search Algorithm for Relating Swelling Potentiality Using Index Geotechnical Properties: A Case Study at El Sherouk City, Egypt

Abdelaziz El Shinawi <sup>1</sup>, Rehab Ali Ibrahim <sup>2</sup>, Laith Abualigah <sup>3</sup>, Martina Zelenakova <sup>4,\*</sup>  
and Mohamed Abd Elaziz <sup>2,5,6,7</sup>

<sup>1</sup> Environmental Geophysics Lab (ZEGL), Geology Department, Faculty of Science, Zagazig University, Zagazig 44519, Egypt; geoabdelaziz@yahoo.com

<sup>2</sup> Department of Mathematics, Faculty of Science, Zagazig University, Zagazig 44519, Egypt; rehab100r@yahoo.com (R.A.I.); abd\_el\_aziz\_m@yahoo.com (M.A.E.)

<sup>3</sup> Faculty of Computer Sciences and Informatics, Amman Arab University, Amman 11953, Jordan; Aligah.2020@gmail.com

<sup>4</sup> Department of Environmental Engineering, Faculty of Civil Engineering, Technical University of Kosice, 04200 Kosice, Slovakia

<sup>5</sup> Faculty of Computer Science & Engineering, Galala University, Suze 435611, Egypt

<sup>6</sup> Artificial Intelligence Research Center (AIRC), Ajman University, Ajman P.O. Box 346, United Arab Emirates

<sup>7</sup> School of Computer Science and Robotics, Tomsk Polytechnic University, Tomsk 634050, Russia

\* Correspondence: martina.zelenakova@tuke.sk



**Citation:** El Shinawi, A.; Ibrahim, R.A.; Abualigah, L.; Zelenakova, M.; Abd Elaziz, M. Enhanced Adaptive Neuro-Fuzzy Inference System Using Reptile Search Algorithm for Relating Swelling Potentiality Using Index Geotechnical Properties: A Case Study at El Sherouk City, Egypt. *Mathematics* **2021**, *9*, 3295. <https://doi.org/10.3390/math9243295>

Academic Editor: Georgios Tsekouras

Received: 21 November 2021

Accepted: 14 December 2021

Published: 18 December 2021

**Publisher's Note:** MDPI stays neutral with regard to jurisdictional claims in published maps and institutional affiliations.



**Copyright:** © 2021 by the authors. Licensee MDPI, Basel, Switzerland. This article is an open access article distributed under the terms and conditions of the Creative Commons Attribution (CC BY) license (<https://creativecommons.org/licenses/by/4.0/>).

**Abstract:** The swelling potentiality is a vital property of fine-grained soils strictly related to the index properties and chemical composition. The integration of machine learning techniques and geotechnical parameters provided a new integrative approach for predicting the free swelling index (FSI) and the swelling pressure (SP). In this paper, an adaptive neuro-fuzzy inference system (ANFIS) using named Reptile Search Algorithm (RSA) is presented to predict the swelling potentiality for fine-grained soils in the foundation bed at El Sherouk city, Egypt. The developed predictive model, named RSA-ANFIS, used as input measured 108 natural fine-grained soil samples of index geotechnical parameters and chemical composition as input data and the measured data of the free swelling index and the swelling pressure as output data. To justify the performance of the developed model, a comparative study was carried out, and the results show that the developed RSA-ANFIS has a high performance over the competitive methods in terms of coefficient of determination, root mean square error (RMSE), and mean absolute error (MAE). This new integrative approach is considered at the highly developed stage to predict and improve the analysis of multi-parameter soil behavior and could be applied in other objective variable datasets.

**Keywords:** machine learning techniques; liquid limit; clay fraction; swelling potentiality

## 1. Introduction

Globally, swelling soils are considered as the more common problematic soils worldwide, and the investigation of these soils has a high priority challenge. These soils are composed of fine-grained soils. Therefore, these soils are essential in different geotechnical practices. Consequently, the damages in swelling soils due to changing moisture contents are a common problem, and the payments for this problem are reported frequently and cannot be neglected. In general, the swelling potentiality for soils is considered a vital property of fine-grained soils characterization.

Accordingly, the categorization of swelling potentiality can be undertaken by a lot of methods [1]. Furthermore, volume changes are assessed by empirical methods with various geotechnical parameters such as Atterberg limits. The Oedometer test signifies

supplementary direct methods of assessing volume changes; nevertheless, they are expensive and time-consuming, using disturbed samples only, which are expensive and difficult to obtain [2]. However, the mineralogical and chemical composition effect are not clarified and explicated on the index geotechnical properties of the clayey soils with the new and effective methods [1,3,4]. At the moment, greater attention has been given to empirical investigations of the swelling behavior of compacted and natural soils. In contrast, the effects of mineralogical and chemical composition are not clarified and explicated on index geotechnical properties of the clayey soils with the new and effective methods [5–7].

Recently, there has been increasing interest in integrating artificial neural networks (ANNs) and fuzzy logic systems, resulting in an adaptive neuro-fuzzy inference (ANFIS) system. This system combines the strength of fuzzy systems with the high learning capacity of ANN [8]. The great performance of the ANFIS for predicting the swelling potentiality has been shown in an increasing body of literature, including the works of [9–11]. However, the performance of the ANFIS model depends on the value of its parameter, and this can lead to degradation in the quality of the output when they are not determined to be optimal. This motivated us to provide an alternative version of ANFIS using a new metaheuristic (MH) technique named Reptile Search Algorithm (RSA). This MH technique (i.e., RSA), emulates the behavior of a reptile to find its prey. In general, RSA has been applied to solve different optimization problems, as in [12]. According to this behavior, we used RSA to enhance the efficiency of ANFIS through determining the best configuration of ANFIS that can lead to increasing the prediction accuracy. Many researchers have related swelling with the index geotechnical properties of clayey soils [13–16]. However, few recent studies try to predict the swelling potentiality [17,18]. On the other hand, the empirical methods that assess volume changes in terms of simple soil properties are relatively simple, inexpensive, and accepted as simple indicator methods. This study was conducted to predict the free swelling index and swelling pressure of clay soils. For study persistence, the comparative study of the RSA-ANFIS was applied to relate the free swelling index (FSI) and the swelling pressure (SP) with datasets measured and the accompanied model with multi-parameters of tested soil samples under the same conditions. Perceptibly, such an inquiry is essential for engineers to verify the proper empirical relations. The main contributions of this study can be summarized as follows:

- 1- Propose a modified ANFIS model and apply it to improve the prediction of the free swelling index (FSI) and the swelling pressure (SP).
- 2- Enhance the performance of ANFIS using the operators of the new MH technique named Reptile Search Algorithm (RSA).
- 3- Apply the developed prediction model, named RSA-ANFIS, to real collected data from El Sherouk City, Egypt.

The paper is organized as follows: In Section 2, the Materials and Methods are introduced. Section 3 presents the steps of prediction of the RSA-ANFIS model. The results and discussion are given in Section 4. Finally, the conclusion and future work are given in Section 5.

## 2. Materials and Methods

### 2.1. Geotechnical Data

Expansive soils are a combination of chemical and mineral composition and suffer unpredictable volume change potentiality. The swelling properties of expansive soils are accompanied by physical, index properties, and chemical composition. Here, 36 disturbed high plastic clay samples were collected from the Miocene foundation level at El Shorouq city. At this point, the physical properties of these samples were conducted including water content, bulk density, and particle-size distribution. Atterberg limits were measured for all samples [19]. Regarding the Unified Soils Classification [20], the soil samples were classified.

The experimental program was applied according to the procedure of ISO/IEC 17025:2017 in Soil Research Unit (SRU) at Zagazig Environmental Geophysics Labora-

tory (ZEGL). In addition, for uncertainty estimation, each test is to be performed (5) times, First, we specified the uncertainty sources, such as the environmental conditions of the lab. The major oxides of the tested samples were carried out using the ICP-OES technique available at the Groundwater Research Institute, Al-Kanater Al-Khayria, Egypt. The Free Swell Index (FSI) test was performed as one of the more important direct methods to determine the free swell value. The FSI is calculated using the following equation

$$FSI = (VL - VS)/VS \times 100$$

where VS is the volume of a given mass (10 g) of fully dried experimental soil (volume is measured by reading the graduation mark up to which dry soil occupies in the cylinder), and VL is the final equilibrium volume of this soil when it is immersed in water in the 100 mL graduated cylinder.

The swelling pressure was performed (Figure 1) using an Oedometer test by controlled a sample laterally and axially with increasing stress [20].

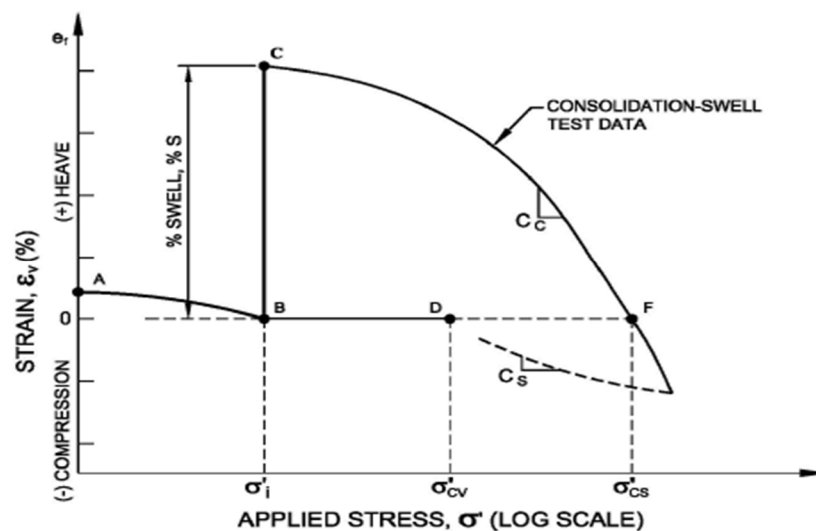


Figure 1. Methodologic scheme of the Oedometer test [20].

As a final point, the results were analyzed to propose suitable regression equations recommended for predicting the swelling potentiality regarding the index properties. Therefore, it was proposed by simple geotechnical parameters to give a preliminary estimate of potential swelling, and if this was extensive, further testing such as the Oedometer test could be carried out.

2.2. Adaptive Neuro-Fuzzy Inference System (ANFIS) and the Honey Badger Algorithm Are Discussed Briefly in this Section

2.2.1. Adaptive Neuro-Fuzzy Inference System

The ANFIS system is considered as a type of ANN that depends on the Takagi–Sugeno fuzzy inference system, which combines ANN and fuzzy logic in one framework to benefit from their advantages [21]. The learning of ANFIS can be accomplished without the need for professional knowledge due to its learning potential. Rules make it possible to analyze both qualitative and quantitative data, and they are simple enough to make the reasoning behind the model’s outcomes understandable [8]. The membership functions  $\mu_A(x) \in [0, 1]$  can be used to express the fuzzy system component in ANFIS. These functions have ability to change the behavior of the input  $x$  into a membership degree between [0, 1].

The following is a list of the outputs ( $f_i$ ) for the given scenario, which has two rules with two inputs ( $x$  and  $y$ ):

Rule 1 : If  $x$  is A1 and  $y$  is B1 then  $f_1 = p_1x + q_1y + r_1$

Rule 2 : If  $x$  is  $A_2$  and  $y$  is  $B_2$  then  $f_2 = p_2x + q_2y + r_2$ ,

where  $A_i$  and  $B_i$  stand for the fuzzy sets and  $p_j, q_j, r_j$  denote the consequent parameters that are required to determine their values over the training stage.

Fuzzification, inference, normalization, consequence, and output are the five layers that make up ANFIS' architecture. In Figure 2, these layers are depicted.

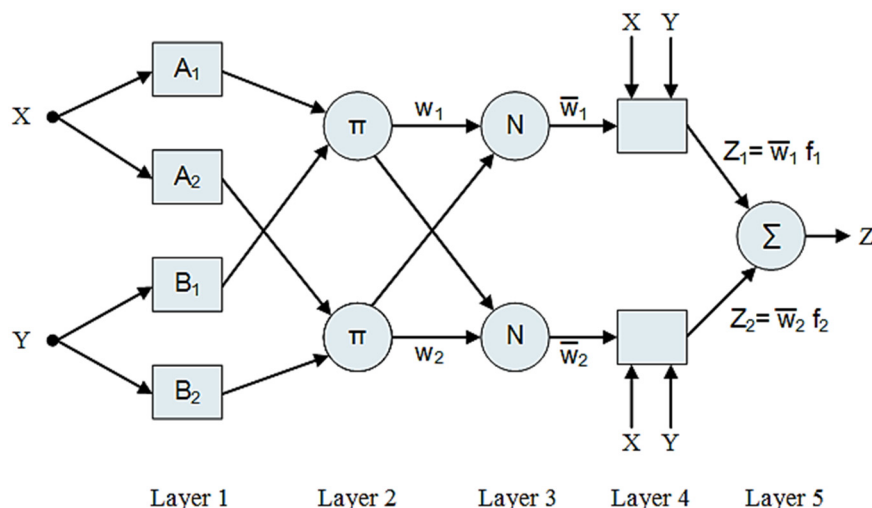


Figure 2. Structure of ANFIS.

The following include the description of the five layers of ANFIS:

Layer 1: The first layer's parameters are known as "premise parameters," and each node in this layer generates a fuzzy membership degree. Assume  $O_{ij}$  is the  $i$ th level and  $j$ th node for the first level:

$$O_{1j} = \mu_{A_j}(x) \text{ for } j = 1, 2, O_{1j} = \mu_{B_j}(x) \text{ for } j = 3, 4. \tag{1}$$

In Equation (1),  $\mu_{A_j}(x)$  and  $\mu_{B_j}(x)$  stand for the fuzzy membership function (MF).  $A_j$  and  $B_j$  stand for the fuzzy sets. The Gaussian MF (GMF) using a Sugeno-type fuzzy inference system is applied, and it has the following formula:

$$MF_{ij} = \exp \left[ - \left( \frac{x - \bar{x}}{\sqrt{2\sigma^2}} \right)^2 \right] \text{ for } i = 1, \dots, nj = 1 \dots, m. \tag{2}$$

where  $\bar{x}$  and  $\sigma^2$  refer to the average and variance of the GMF, respectively.

Layer 2: The nodes that belong to the second layer use multiplication to calculate the firing strength for each rule:

$$O_{2j} = w_j = \mu_{A_j}(x) * \mu_{B_j}(x) \text{ for } j = 1, 2. \tag{3}$$

Layer 3: The main aim of this layer is to compute the normalization of the firing strength ( $O_{3j}$ ) as:

$$O_{3j} = \bar{w}_j = \frac{w_j}{(w_1 + w_2)} \text{ for } j = 1, 2. \tag{4}$$

Layer 4: The output of this layer ( $O_{4j}$ ) depends on the  $\bar{w}_j$  and the consequent parameters. It is computed as:

$$O_{4j} = \bar{w}_j f_j = \bar{w}_j (p_j x + q_j y + r_j) \text{ for } j = 1, 2. \tag{5}$$

Layer 5: The output of fifth layer is the output of ANFIS, and it is computed as:

$$O_{5j} = overalloutput = \sum_j \bar{w}_j f_j = \frac{\sum_j w_k f_k}{\sum_j w_k} \text{ for } k = 1, 2. \tag{6}$$

### 2.2.2. Reptile Search Algorithm (RSA)

In [12], a new meta formula named Reptile Search Algorithm (RSA) was introduced, which simulates the hunting behavior of reptiles. The first step in RSA is to generate a set of solutions using the following formula [12]:

$$x_{ij} = rand \times (UB - LB) + LB, \quad j = 1, 2, \dots, n \tag{7}$$

where *rand* stands for a random value. *LB* and *UB* refer to the boundaries of the search domain.

$$x_{(i,j)}(t + 1) = \begin{cases} Best_j(t) \times -\eta_{(i,j)}(t) \times \beta - R_{(i,j)}(t) \times rand, & t \leq \frac{T}{4} \\ Best_j(t) \times x_{(r_1,j)} \times ES(t) \times rand, & t \leq 2\frac{T}{4} \text{ and } t > \frac{T}{4} \end{cases} \tag{8}$$

where the parameter  $\beta$  is used to control the performance of exploration.  $x_{(r_1,j)}$  stands for a random solution at the  $j$ th value.  $r_1$  stands for a random value.  $Best_j(t)$  represents the  $j$ th value of the best at iteration  $t$ .  $rand \in [0, 1]$  represents a random number, and  $T$  is the total number of generations.

In addition,  $R_{(i,j)}$  is the Reduce function, which is used to decrease the search region and it is formulated as:

$$R_{(i,j)} = \frac{Best_j(t) - x_{(r_2,j)}}{Best_j(t) + \epsilon} \tag{9}$$

In addition, the Evolutionary Sense ( $ES(t)$ ) that defined in Equation (3) represents the probability ratio, which decreased from 2 to  $-2$  over the iterations, and it is defined as:

$$ES(t) = 2 \times r_3 \times \left(1 - \frac{1}{T}\right), \tag{10}$$

where  $r_3 \in [-1, 1]$  stands for a random integer number.

$\eta_{(i,j)}$  stands for to the hunting operator at the  $j$ th value of the  $i$ th solution, and it is computed as

$$\eta_{(i,j)} = Best_j(t) \times P_{(i,j)} \tag{11}$$

$P_{(i,j)}$  is the percentage difference between the  $j$ th value of the best solution and its corresponding value in the current solution. It is defined as:

$$P_{(i,j)} = \alpha + \frac{x_{(i,j)} - M(x_i)}{Best_j(t) \times (UB_{(j)} - LB_{(j)}) + \epsilon} \tag{12}$$

In Equation (7),  $\alpha$  dontes a sensitive parameter that controls the exploration performance.  $M(x_i)$  stands for the average solutions, which is defined as:

$$M(x_i) = \frac{1}{n} \sum_{j=1}^n x_{(i,j)} \tag{13}$$

Moreover, the solution can update their value during the exploitation phase using the following formula:

$$x_{(i,j)}(t + 1) = \begin{cases} Best_j(t) \times P_{(i,j)}(t) \times rand, & t \leq 3\frac{T}{4} \text{ and } t > 2\frac{T}{4} \\ Best_j(t) - \eta_{(i,j)}(t) \times \epsilon - R_{(i,j)}(t) \times rand, & t \leq T \text{ and } t > 3\frac{T}{4} \end{cases} \tag{14}$$

### 3. Proposed Model

Figure 3 depicts the framework of the developed model to predict the swelling potentiality. In general, the developed approach is based on improving the performance of ANFIS based on the operators of the RSA algorithm that is used to identify the appropriate ANFIS parameters. The initial stage in the RSA-ANFIS is to preprocess the data by splitting it into two sets: training (70%) and testing (30%). The next stage is to create initial configurations that reflect the RSA population, with each configuration based on ANFIS settings. Then, the quality of each configuration ( $X_i$ ) is evaluated by computing the following fitness value ( $Fit$ ) that is defined as the root mean square error (RMSE).

$$Fit = \sqrt{\frac{\sum_{i=1}^{NS} (y_i - \hat{y}_i)^2}{NS}} \tag{15}$$

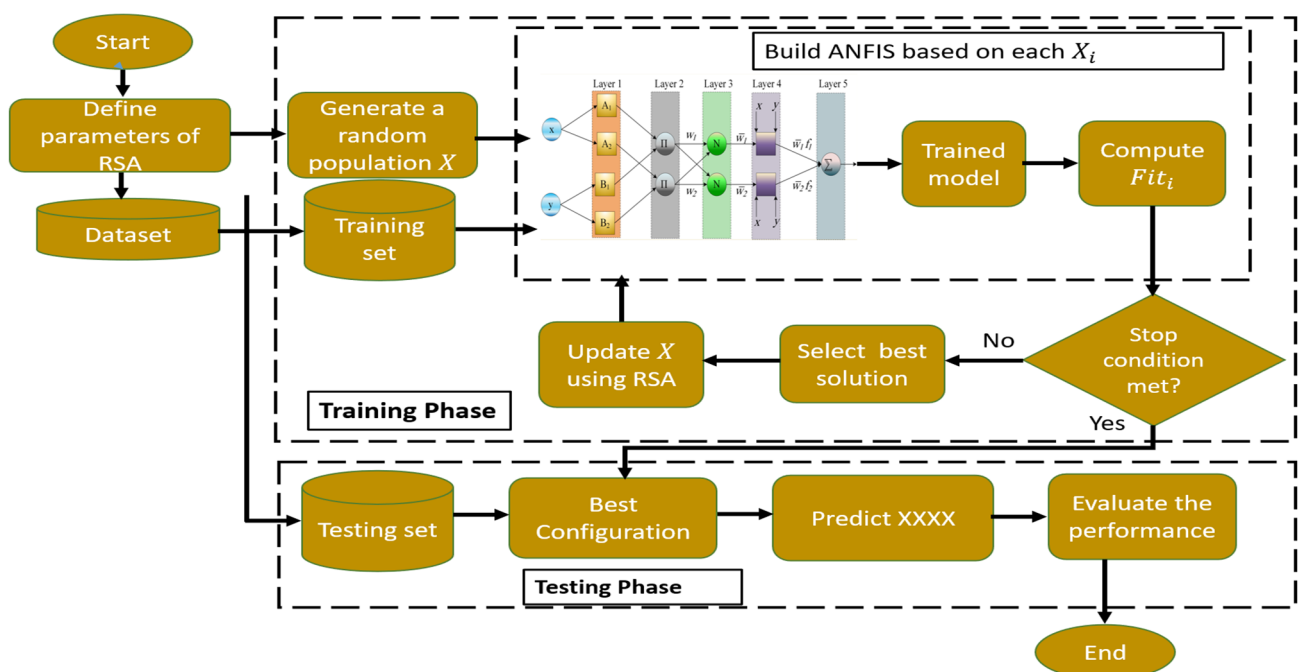


Figure 3. Steps of RSA-ANFIS.

In Equation (14),  $\hat{y}_i$  represents the predicted output of ANFIS using the current  $X_i$  and  $y_i$  is the experimental output. The process after that is to determine the best configuration of the ANFIS (i.e.,  $x^{prey}$ ), which has the smallest fitness value. The next step is to update the value of the other configurations according to the steps of RSA until it reached the stop terminal. When the best configuration ( $x^{prey}$ ) is returned, the terminal condition is satisfied, and the testing set is used to assess the performance of the it (i.e.,  $x^{prey}$ ).

### 4. Results and Discussions

#### 4.1. Physical Soil Properties

According to particle size distribution, the collected soil samples have 0–7% gravel, 6–25% sand, 0.64–1.49, 16–41% silts, and 46–60% clay fraction. The initial moisture content ranges between 7.43 and 10.47%, the bulk density ranges from 1.94 to 2.22 g/cm<sup>3</sup>, and the specific gravity values ranges between 2.62 and 2.78. Soils are categorized as loose and occasionally have very close values of specific gravity, and these inclines may be to the same mineralogical composition. Furthermore, the average of the liquid limit, plastic limits, and plasticity index are 62, 25, and 40%, respectively (Figure 4). These samples were inorganic silty clay (CH). These indices revealed that these samples represent semi-plastic solid to hard consistency clays.

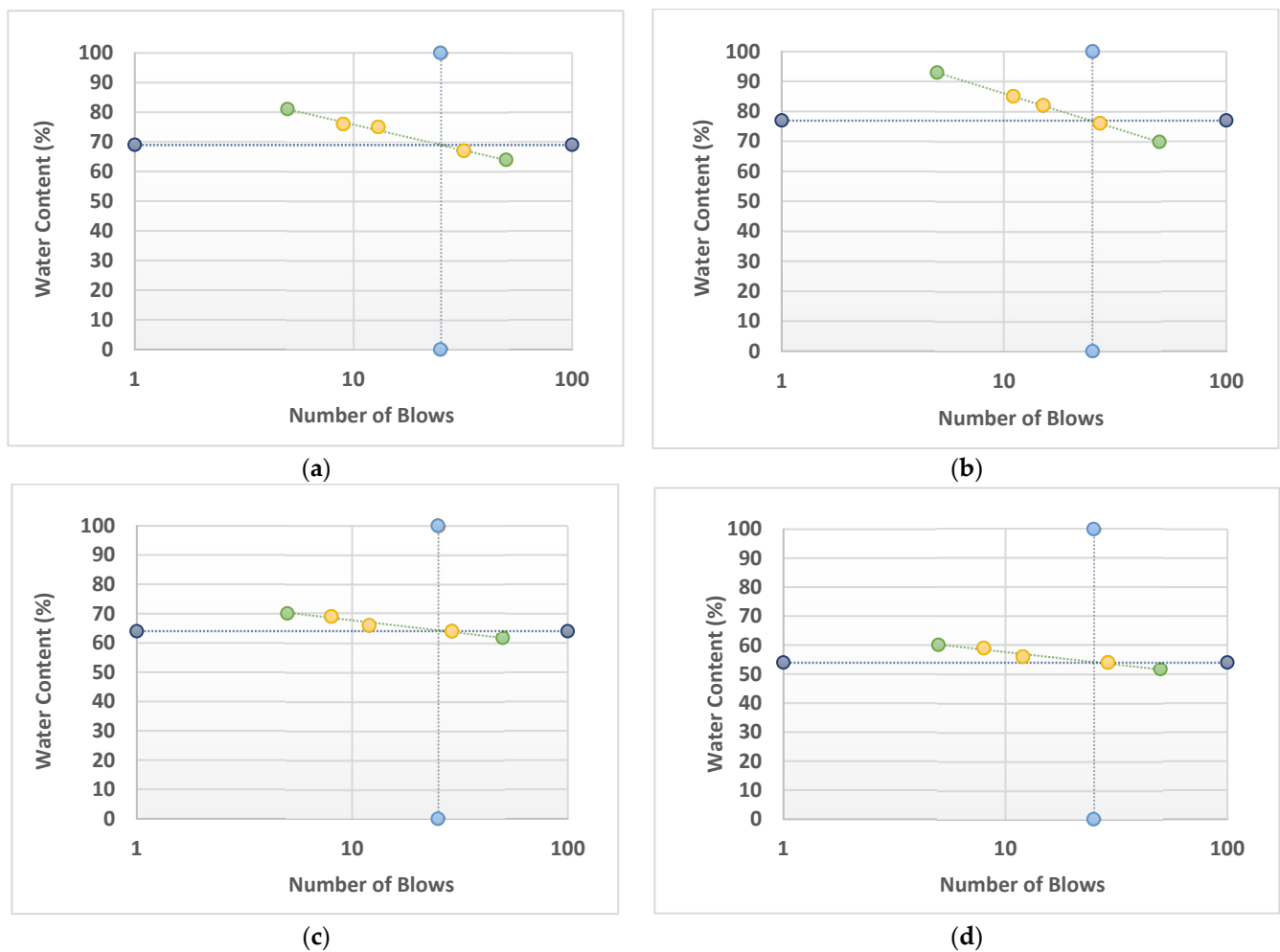


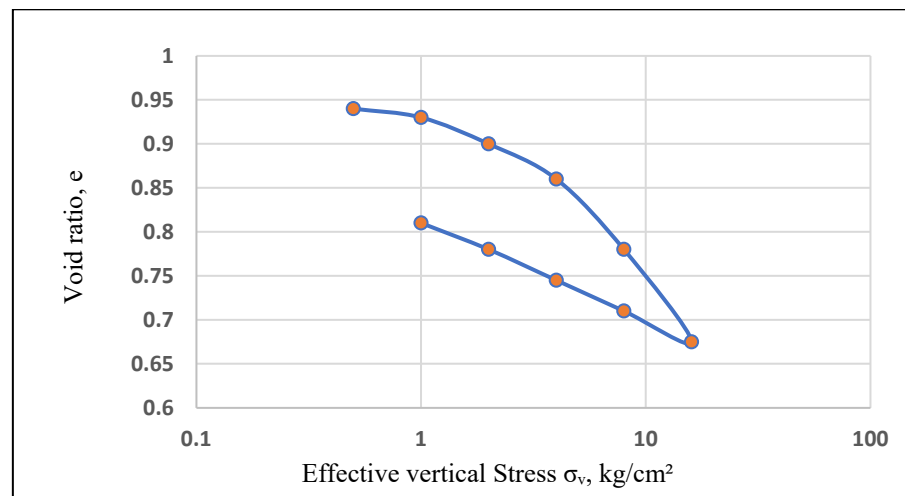
**Figure 4.** Flow curve of liquid limit ( $W_L$ ) test results (examples a–d) for high plastic samples (CH) of shallow marine clays according to ASTM D 4318, 2010.

#### 4.2. Mineralogical and Chemical Composition

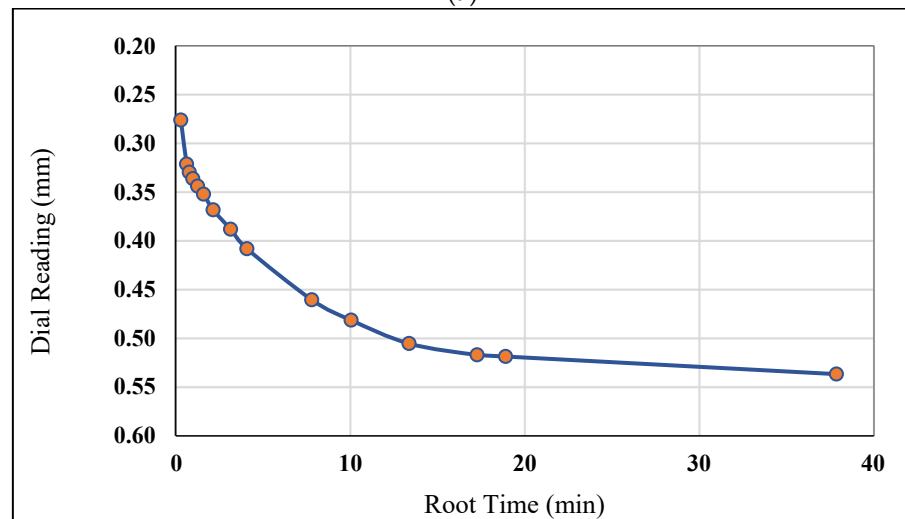
The high plastic clays are composed of Smectite as a major clay mineral with percentages ranges from 62.68 to 77.48% and kaolinite as low as 22.52 to 37.32%. Additionally, the mineralogical composition of these clays contains non-clay minerals such as quartz, gypsum, halite, and calcite (Abdullah et al., 2009). In the present study, the chemical analysis revealed the  $\text{SiO}_2$  content with the highest percentage and the average value of 40%. The high content of  $\text{SiO}_2$  attains that it is derived from sand and silt fraction. In contrast,  $\text{Al}_2\text{O}_3$  content is presented with lower percentages with an average value of 20%.  $\text{Al}_2\text{O}_3$  content in negative relation with  $\text{SiO}_2$  indicates different sources of these oxides and ionic substitution of Ca, Na with Al in the clay mineral structure. In addition, there are low percentages of MgO, CaO, and  $\text{Na}_2\text{O}$  oxides with average values of 2.34%, 1.09%, and 2.04%, respectively.

#### 4.3. Swelling Characteristics

The expansive properties of high plastic clays were identified by measuring both the free swelling and swelling pressure. The free swelling index is 33–130%. On the other hand, the swelling pressure values range between 1.1 and 4.1 MPa. Meanwhile, the swelling index values are very close to each other, ranging from 0.112 to 0.117, and this reflects the homogeneity of the high plastic clay soil. The swelling index ( $C_s$ ) and void ratio ( $e$ ) average values are 0.115 and 0.923, respectively (Figure 5).



(a)



(b)

**Figure 5.** (a) Void ratio vs. log P curve and (b) Compression-square root time curve of representative sample.

#### 4.4. Results Using Machine Learning Method

##### Model Evaluation Criteria

To assess the ability of the developed method to predict the free swell index and the swelling pressure efficiently, a set of performance measures are used: for example, the root mean square error (RMSE), mean absolute error (MAE), and coefficient of determination  $R^2$ . The definition of these measures is given in Equations (16)–(18).

$$R^2 = \frac{\left(\sum_{i=1}^{n_s} (d_i - \bar{d})(y_i - \bar{y})\right)^2}{\sum_{i=1}^{n_s} (d_i - \bar{d})^2 \times \sum_{i=1}^{n_s} (y_i - \bar{y})^2} \tag{16}$$

$$RMSE = \sqrt{\frac{1}{n_s} \sum_{i=1}^{n_s} (d_i - y_i)^2} \tag{17}$$

$$MAE = \frac{1}{n_s} \sum_{i=1}^{n_s} |d_i - y_i| \tag{18}$$

The structure of the ANFIS consists of five layers as described in Section 2.2.1. In addition, the parameters of RSA, Ant Lion Optimizer (ALO), and Gray Wolf Optimizer

(GWO) are set according to the original implementation of each of them. For fair comparison between them, we unify the common parameters between them, such as the number of solutions is ten and the number of iterations is 15 iterations. In addition, each algorithm is conducted 25 independent times to assess its performance.

To justify the performance of the developed RSA-ANFIS, it is compared with other two well-known metaheuristic techniques that are used to improve the ANFIS model. These methods are named ALO-ANFIS and GWO-ANFIS. The comparison results are given in Table 1 and Figures 6 and 7. It can be noticed from these results that the developed RSA-ANFIS has a high coefficient of determination  $R^2$ , which indicates the high correlation with the Free Swelling Index. It is followed by ALO-ANFIS, while the GWO-ANFIS is the less efficient one. According to the RMSR indicator, it can be noticed that the RMSE of RSA-ANFIS is the smallest one, which refers to the similarity between the predicted value using RSA and the original one. The similar observation can be noticed from the value of MAE obtained for each algorithm (i.e., RSA, ALO, and GWO). From these measures, it can be seen that the combination between the RSA and ANFIS leads to enhancing the prediction process. The same observation can be reached from Figure 7.

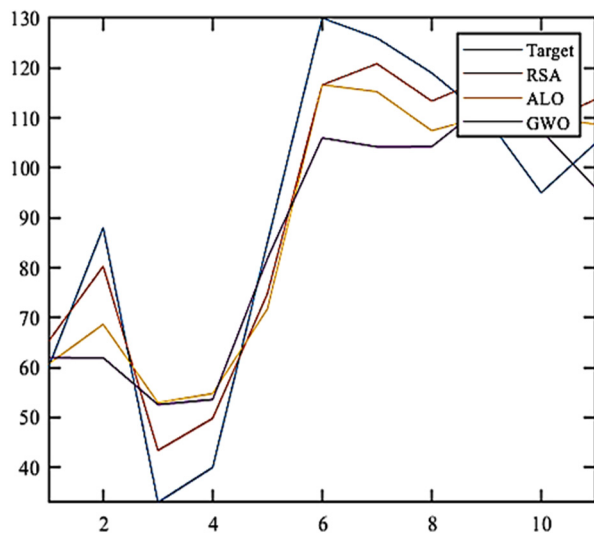
**Table 1.** Comparison results between RSA-ANFIS and other models.

	Free Swelling Index			Swelling Pressure		
	RSA	ALO	GWO	RSA	ALO	GWO
$R^2$	0.990	0.982	0.972	0.955	0.941	0.944
RMSE	9.353	12.925	15.887	0.580	0.667	0.650
MAE	8.911	11.179	13.582	0.487	0.579	0.550

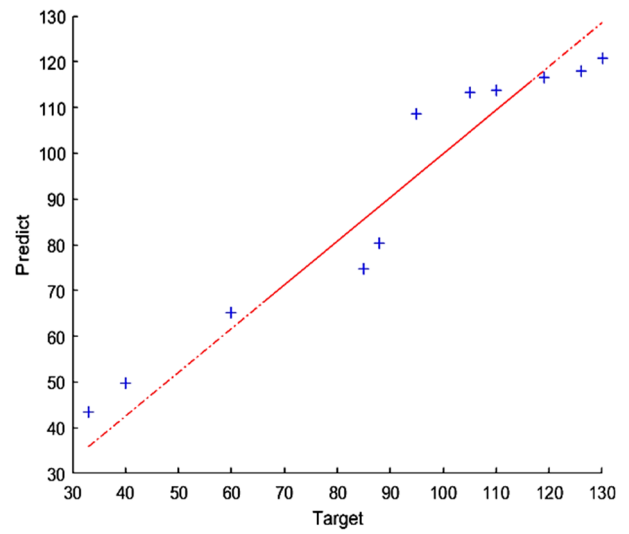
In addition, we evaluate the influence of changing the size training and testing sets on the performance of the developed RSA-ANFIS. The results are given in Table 2, where the size of the testing set is 30%, 10%, and 50%. From these results, it can be noticed that as expected, with increasing the size of the training set, the performance of the developed method increases.

**Table 2.** Influence of changing the size of the testing set.

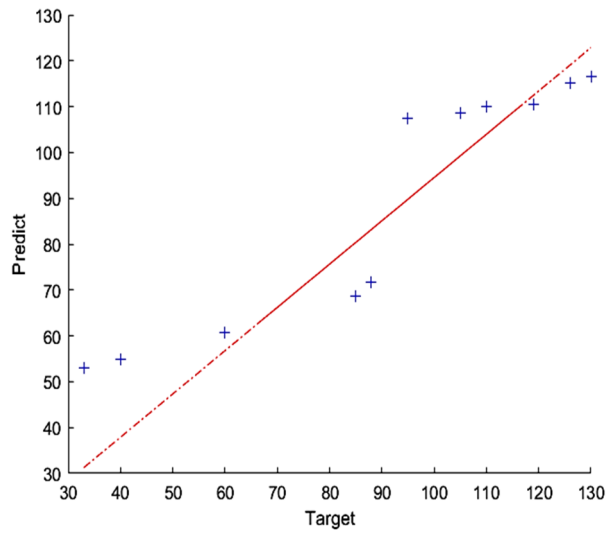
	Free Swelling Index			Swelling Pressure		
	70–30	90–10	50–50	70–30	90–10	50–50
$R^2$	0.990	0.999	0.978	0.955	0.974	0.931
RMSE	9.353	3.798	13.104	0.580	0.492	0.666
MAE	8.911	3.127	10.010	0.487	0.424	0.562



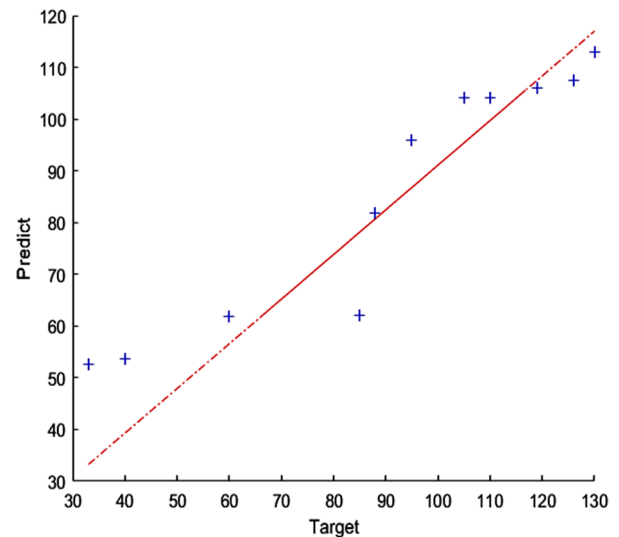
(A)



(B)



(C)



(D)

**Figure 6.** The predicted value obtained by RSA-ANFIS, ALO-ANFIS, and GWO-ANFIS using the Free Swelling Index (Target). (A) Predicted values using the three algorithms and measured data, (B) QQ-plot for RSA-ANFIS, (C) QQ-plot for ALO-ANFIS, (D) QQ-plot for GWO-ANFIS.

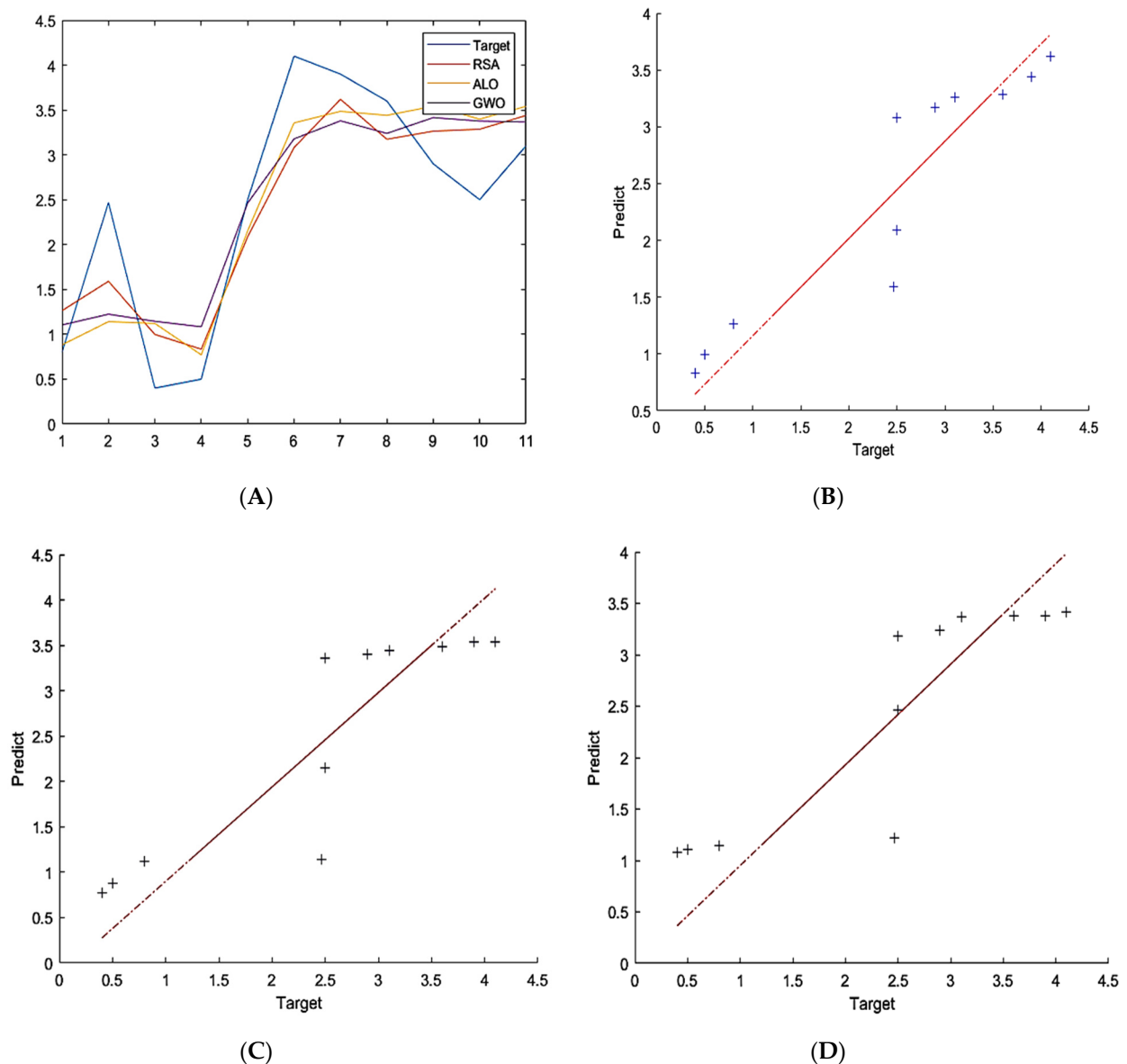


**Figure 7.** The predicted value obtained by RSA-ANFIS, ALO-ANFIS, and GWO -ANFIS using swelling pressure (Target). (A) Predicted values using the three algorithms and measured data, (B) QQ-plot for RSA-ANFIS, (C) QQ-plot for ALO-ANFIS, (D) QQ-plot for GWO-ANFIS.

### 5. Conclusions

The fine-grained soils are distributed worldwide, and the classification of such soils has a high priority challenge. Therefore, these soils are considered as problematic soils, and their characterization is essential anywhere in different geotechnical engineering practices. In the present study, machine learning techniques were conducted to predict the swelling potentiality in two main outputs, Free Swelling Index and the swelling pressure using multi-parameters of the index geotechnical properties and the chemical composition as an input parameter. Consequently, the clayey soils are classified as high plastic (CH). Firstly, the liquid limit, plastic limit, plasticity index and clay fraction of the studied shallow marine clays average values are 62, 25, 40, and 55%, respectively. Secondly, the measured chemical oxides percentages ( $Al_2O_3$ ,  $SiO_2$ ,  $CaO$ ,  $MgO$ , and  $Na_2O$ ) were 40, 20, 2.34, 1.09, and 2.04%, respectively. The Free Swelling Index is 33–130%. On the other hand, the swelling pressure values range between 1.1 and 4.1 MPa. Then, a comparative study of machine learning algorithms (i.e., RSA-ANFIS, ALO-ANFIS, and GWO-ANFIS) with the measured datasets

was used to predict the swelling potentiality in two output parameters. For this purpose, the model was built to compare their enactment. Consequently, the model providing the best performance according to the  $R^2$  coefficient was approved. It can be noticed from these results that the developed RSA-ANFIS has a high coefficient of determination,  $R^2$  (0.99), which indicates the high correlation with the target of free swelling index and 0.96 for the swelling pressure output. It was followed by ALO-ANFIS, while GWO-ANFIS is the less efficient one. From these measures, it can be seen that the combination between the RSA and ANFIS leads to enhancing the prediction process. On the whole, this study introduces a new integration for prediction using multi-parameters to predict the swelling potentiality and soil behavior. In addition, the usage of machine learning techniques will provide high quality and precise predicted values supported by a large amount of data.

**Author Contributions:** A.E.S.; Data curation, M.A.E., L.A. and R.A.I.; Formal analysis, M.Z.; Funding acquisition, R.A.I.; Investigation, L.A., M.A.E. and R.A.I.; Methodology, M.A.E.; Supervision, A.E.S.; Writing, A.E.S., L.A., M.Z., M.A.E.; Revising. All authors have read and agreed to the published version of the manuscript.

**Funding:** This research received no external funding.

**Institutional Review Board Statement:** Not applicable.

**Informed Consent Statement:** Not applicable.

**Data Availability Statement:** Not applicable.

**Acknowledgments:** We are grateful to the Zagazig University Environmental Geophysics Lab for helping us to perform the laboratory testing. This work was supported by the Slovak Research and Development Agency under the Contract no. APVV-20-0281. This work was supported by project HUSKROUA/1901/8.1/0088 Complex flood-control strategy on the Upper-Tisza catchment area.

**Conflicts of Interest:** The authors declare no conflict of interest.

## Nomenclature

### Acronyms

ANFIS	Adaptive Neuro-Fuzzy Inference System	MH	meta heuristic
RSA	Reptile Search Algorithm	ALO	Ant Lion Optimizer
SP	Swelling Pressure	GWO	Grey Wolf Optimizer
FSI	Free Swelling Index	MAE	Mean Absolute Error
RMSE	Root Mean Square Error	ANNs	artificial neural networks

## References

- Naymushina, O.; El-Shinawi, A. Geotechnical aspects of flood plain deposits in south east Aswan City, Egypt. *J. Eng. Appl. Sci.* **2015**, *10*, 3490–3497.
- Nabih, M.; El Shinawi, A. Qualitative analysis of clay minerals and swelling potential using gamma-ray spectrometry logs: A case study of the Bahariya Formation in the Western Desert, Egypt. *Appl. Radiat. Isot.* **2020**, *166*, 109384. [[CrossRef](#)] [[PubMed](#)]
- Attwa, M.; El Shinawi, A. Geoelectrical and geotechnical investigations at tenth of ramadan City, Egypt—a structure-Based (SB) model application. In Proceedings of the Near Surface Geoscience 2014-20th European Meeting of Environmental and Engineering Geophysics, Athens, Greece, 14–18 September 2014; pp. 1–5.
- Benbouras, M.A.; Petrisor, A.-I. Prediction of Swelling Index Using Advanced Machine Learning Techniques for Cohesive Soils. *Appl. Sci.* **2021**, *11*, 536. [[CrossRef](#)]
- Naymushina, O.S.; Shvartsev, S.L.; Zdvizhkov, M.A.; El-Shinawi, A. Chemical characteristics of swamp waters: A case study in the Tom River Basin, Russia. In Proceedings of the Water-Rock Interaction—Proceedings of the 13th International Conference on Water-Rock Interaction, WRI-13, Guanajuato, Mexico, 16–20 August 2010; pp. 955–958.
- Mawlood, Y.I.; Hummadi, R.A. Large-Scale Model Swelling Potential of Expansive Soils in Comparison with Oedometer Swelling Methods. *Iran. J. Sci. Technol. Trans. Civ. Eng.* **2020**, *44*, 1283–1293. [[CrossRef](#)]
- Nosair, A.M.; Shams, M.Y.; AbouElmagd, L.M.; Hassanein, A.E.; Fryar, A.E.; Salem, H.S.A. Predictive model for progressive salinization in a coastal aquifer using artificial intelligence and hydrogeochemical techniques: A case study of the Nile Delta aquifer, Egypt. *Environ. Sci. Pollut. Res.* **2021**. [[CrossRef](#)] [[PubMed](#)]

8. Atsalakis, G.S.; Atsalaki, I.G.; Zopounidis, C. Forecasting the success of a new tourism service by a neuro-fuzzy technique. *Eur. J. Oper. Res.* **2018**, *268*, 716–727. [[CrossRef](#)]
9. Al-qaness, M.A.A.; Fan, H.; Ewees, A.A.; Yousri, D.; Elaziz, M.A. Improved ANFIS model for forecasting Wuhan City Air Quality and analysis COVID-19 lockdown impacts on air quality. *Environ. Res.* **2021**, *194*, 110607. [[CrossRef](#)] [[PubMed](#)]
10. AlRassas, A.M.; Al-Qaness, M.A.A.; Ewees, A.A.; Ren, S.; Elaziz, M.A.; Damaševičius, R.; Krilavičius, T. Optimized ANFIS Model Using Aquila Optimizer for Oil Production Forecasting. *Processes* **2021**, *9*, 1194. [[CrossRef](#)]
11. Zayed, M.E.; Zhao, J.; Li, W.; Elsheikh, A.H.; Elaziz, M.A. A hybrid adaptive neuro-fuzzy inference system integrated with equilibrium optimizer algorithm for predicting the energetic performance of solar dish collector. *Energy* **2021**, *235*, 121289. [[CrossRef](#)]
12. Abualigah, L.; Elaziz, M.A.; Sumari, P.; Geem, Z.W.; Gandomi, A.H. Reptile Search Algorithm (RSA): A nature-inspired meta-heuristic optimizer. *Expert Syst. Appl.* **2021**, 116158. [[CrossRef](#)]
13. Reddy, P.S.; Mohanty, B.; Rao, B.H. Investigations for Chemical Parameters Effect on Swelling Characteristics of Expansive Soils. *KSCE J. Civ. Eng.* **2021**, *25*, 4088–4105. [[CrossRef](#)]
14. Çimen, Ö.; Keskin, S.N.; Yıldırım, H. Prediction of Swelling Potential and Pressure in Compacted Clay. *Arab. J. Sci. Eng.* **2012**, *37*, 1535–1546. [[CrossRef](#)]
15. Wójcik, E.; Gawriuczenkow, I. Determination of swell index and swelling pressure from suction tests—A case study of Neogene clays from Warsaw (Poland). *Geol. Q.* **2017**. [[CrossRef](#)]
16. Seif, E.-S.S.A. Geotechnical hazardous effects of municipal wastewater on plasticity and swelling potentiality of clayey soils in Upper Egypt. *Int. J. Geo-Eng.* **2017**, *8*, 1. [[CrossRef](#)]
17. Işık, N.S. Estimation of swell index of fine grained soils using regression equations and artificial neural networks. *Sci. Res. Essays* **2009**, *4*, 1047–1056.
18. Alptekin, A.; Taga, H. Prediction of Compression and Swelling Index Parameters of Quaternary Sediments from Index Tests at Mersin District. *Open Geosci.* **2019**, *11*, 482–491. [[CrossRef](#)]
19. ASTM Committee D-18 on Soil and Rock. In *Standard Test Methods for Liquid Limit, Plastic Limit, and Plasticity Index of Soils*; ASTM international: West Conshohocken, PA, USA, 2010.
20. *ASTMD2435M-11. Standard Test Methods for One-Dimensional Consolidation Properties of Soils Using Incremental Loading*; ASTM International: West Conshohocken, PA, USA, 2020. [[CrossRef](#)]
21. Yaghoobi, A.; Bakhshi-Jooybari, M.; Gorji, A.; Baseri, H. Application of adaptive neuro fuzzy inference system and genetic algorithm for pressure path optimization in sheet hydroforming process. *Int. J. Adv. Manuf. Technol.* **2016**, *86*, 2667–2677. [[CrossRef](#)]